HHS Public Access

Author manuscript

Opt Lett. Author manuscript; available in PMC 2018 April 19.

Published in final edited form as:

Opt Lett. 2017 December 01; 42(23): 4978–4981.

Broadband rotary joint for high-speed ultrahigh-resolution endoscopic OCT imaging at 800 nm

Hyeon-Cheol Park[1], **Jessica Mavadia-Shukla**[1], **Wu Yuan**[1], **Milad Alemohammad**[2], and **Xingde Li**[1,*]

[1]Department of Biomedical Engineering, School of Medicine, Johns Hopkins University, Baltimore, Maryland 21205, USA

[2]Department of Electrical and Computer Engineering, Johns Hopkins University, Baltimore, Maryland 21205, USA

Abstract

We report the development of a broadband rotary joint for high-speed ultrahigh-resolution endoscopic optical coherence tomography (OCT) imaging in the 800 nm spectral range. This rotary joint features a pair of achromatic doublets in order to achieve broadband operation for a 3 dB bandwidth over 150 nm. The measured one-way throughput of the rotary joint is greater than 80%, while the fluctuation of the double-pass coupling efficiency during 360 deg rotation is less than ±5% at a near video-rate speed of 20 revolutions/s (rps). The rotary joint is used in conjunction with a diffractive-optics-based endoscope and 800 nm spectral domain OCT system and achieved an ultrahigh axial resolution of ~2.4 μm in air. The imaging performance is demonstrated by 3D circumferential imaging of a mouse colon *in vivo*.

Optical coherence tomography (OCT) is a recently developed technology that enables direct visualization of tissue structures noninvasively with microscopic resolution and an imaging depth of a few millimeters [1]. With the advances of endoscopic OCT over the past decade, this technology is now being translated to clinical settings, especially for imaging luminal organs, such as airway, colon, and esophagus [2–5]. Most endoscopic OCT systems that have been developed so far operate at 1300 nm and provide an axial resolution around 10 μm [6–10]. However, higher resolution is desired in order to resolve fine tissue structures such as airway smooth muscle, intestinal crypts, or subtle structural changes associated with early stage diseases. In addition, any potential improvement in imaging contrast would also be appreciated.

It is well-known that the axial resolution of the OCT system is determined by the central wavelength and the spectral bandwidth of the light source. Higher resolution can be readily achieved by selecting a shorter central wavelength for a given spectral bandwidth. While conventional endoscopic OCT systems operate at 1300 nm, second-generation 800 nm endoscopic OCT systems can greatly improve the axial resolution from ~10 μm down to a

*Corresponding author: xingde@jhu.edu.

OCIS codes: (170.2150) Endoscopic imaging; (110.4500) Optical coherence tomography; (170.3880) Medical and biological imaging.

few micrometers. Moreover, higher light scattering and lower tissue absorption at 800 nm potentially lead to an improved image contrast, although it may also reduce the light penetration depth. High axial resolution with high contrast at 800 nm has been demonstrated in bench-top systems [11,12]. Compared with 1300 nm, however, managing chromatic aberration over a broad spectrum around 800 nm becomes more challenging, particularly for the endoscopic OCT system.

The past few years have witnessed continued efforts to achieve a portable, ultrahigh-resolution 800 nm endoscopic OCT system. First, portable ultra-broadband light sources such as supercontinuum lasers have become readily available, and their optimal operational conditions have been investigated [13]. Second, an achromatic endoscopic catheter has recently been developed to minimize chromatic aberrations by employing cost-effective diffractive optics at the distal end [14]. Finally, the last required component to realize an ultrahigh-resolution endoscopic OCT system is the scanning unit, which is the fiber-optic rotary joint. A fiber-optic rotary joint is one of the key components for an endoscopic OCT system that enables circumferential scanning of the endoscopic catheter from the proximal end. Broadband fiber-optic rotary joints at 1300 nm are commercially available and have been widely adapted for various endoscopic OCT applications. Recently, a gradient-index (GRIN) lens-based fiber-optic rotary joint has been demonstrated, which achieved an imaging speed of 350 frames per second (fps) [15]. In contrast, the operational spectral bandwidth in commercial 800 nm rotary joints is limited due to the severe chromatic aberration of the coupling optics, such as a GRIN lens collimator, which, in turn, degrades the resolution afforded by the broadband light source. Moreover, the mode field diameter of a single-mode fiber (SMF) at 800 nm is much smaller than that of a 1300 nm SMF. Therefore, light coupling with a high throughput between a stationary and a rotary SMF in a rotary joint becomes challenging. One method is to directly couple the stationary and rotary bare fibers inside a glass capillary tube filled with index-matching oil [16]. This method provides an excellent coupling throughput of ~90% without compromising spectral bandwidth. However, this design is fundamentally limited in terms of mechanical robustness. Bare fiber ends inside the tube can quickly wear out or get damaged at high speed. Moreover, efficient coupling heavily relies on high-precision flat cleaving of the fibers. Beam scanning by a micromotor at the distal end of an endoscope can be an alternative approach to avoid the use of a fiber-optic rotary joint and the associated challenges with chromatic aberrations at 800 nm; however, this approach is suboptimal, especially for imaging small luminal organs [8–10]. Distal end scanning probes generally have relatively larger diameter and suffer from a compromised field of view due to beam blockage by mechanical structures between optics and micromotor or electrical wires. Moreover, micromotors are expensive and fragile, making it not viable to have disposable distal-scanning probes for clinical use. Therefore, there exists a substantial need for a robust and reliable rotary joint for clinical translation of ultrahigh-resolution endoscopic imaging at 800 nm. In this Letter, we report the development of a broadband and high-speed rotary joint to enable ultrahigh-resolution endoscopic OCT imaging at 800 nm.

Figure 1(a) shows the schematic of the broadband rotary joint. Two identical spherical achromatic doublets with a 4 mm focal length were used to couple light between the stationary and the rotary SMFs over a broadband spectrum with a center wavelength around

820 nm. Several key engineering parameters, including the lateral and angular misalignment and separation between the two lenses, are critical for achieving a sufficient coupling efficiency and a tolerable variation in throughput during full circumferential rotation. Ray tracing simulations were carried out to analyze the engineering tolerance to the above-mentioned parameters. As shown in Fig. 1(b), with a collimated beam waist diameter of 0.87 mm, for example, less than ±5% of the coupling efficiency fluctuation can be achieved within an alignment tolerance of ±85 μm (lateral misalignment) or ±9 mdeg (angular misalignment). The through-put of the rotary joint will also be affected by the distance between the two lenses. However, we still can obtain over 80% of one-way throughput at a maximum separation of 70 mm between the two lenses with 9 mdeg angular misalignment and 85 μm lateral misalignment, as shown in Fig. 1(c). It is noted that large spacing between the two lenses offers the freedom to install additional optical components between the two arms, which make the rotary joint potentially useful for multi-modal or functional imaging.

For precision assembly, each fiber and achromatic lens were preassembled and aligned using customized compact fiver-axis kinematic mounts to ensure beam collimation as well as optical axis alignment. Particularly, the collimated beam waist positions with respect to the two lenses were carefully matched in order to maximize the coupling efficiency. Each fiber/lens assembly was then mounted on a five-axis kinematic mount for alignment between the optical axis and the rotation axis. Two pillow-mounted ball bearings were utilized for high-speed rotation. Considering the worst eccentricity of the bearings (7.5 μm, ISO 492, normal class 6×), the two bearings were press fit on the rotating shaft at least 50 mm apart to maintain maximum run-out of less than ±9 mdeg during the rotation. A short fiber patch cord was also placed inside the shaft with one end connecting to the endoscope catheter via a mating sleeve mounted on the end of the shaft. Finally, circumferential rotation was achieved by a DC motor through a pair of pulleys and a timing belt, where the motor drive was feedback-controlled using three integrated Hall effect sensors for ensuring uniform rotation speed during imaging. After precision assembly and alignment, all the opto-mechanical components were firmly secured with locking screws to ensure the mechanical robustness during the high-speed rotation.

The fluctuation in the double-pass coupling efficiency was measured by connecting a short piece (~5 cm long) of flat cleaved fiber to the rotary arm. The fluctuation of backreflected light intensity from the fiber tip during circumferential scanning was measured to be less than ±2% at a speed of 5 revolution/s (rps). Throughput fluctuation tends to increase with scanning speed due to the additional misalignment caused by an increased centrifugal force within the current suboptimal mechanical design, but it still remains at a level of less than ±5% for a speed up to 20 rps, as shown in Fig. 1(e). It is noted that all fiber ends in the rotary joint were cleaved at an 8 deg angle in order to minimize the backreflection (less than −60 dB). More importantly, the achromatic doublets provide excellent chromatic performance. Figure 1(f) shows the comparison between normalized input and output spectra of the rotary joint measured with the Ti:sapphire laser, which has a central wavelength of ~820 nm and an FWHM bandwidth of ~150 nm. The average one-way throughput is measured to be greater than 80%, and the maximum spectrum variation over the full bandwidth is less than 2%.

The broadband rotary joint was integrated with an ultrahigh-resolution spectral-domain OCT (SD-OCT) system, as illustrated in Fig. 2(a). A broadband Ti:sapphire laser was used as the light source. A home-built linear-in-wavenumber spectrometer, which consists of a grating (1200 lines/mm), a prism, and a line scan charge-coupled device (CCD) camera [Fig. 2(b)], was employed as the detection unit [17]. The CCD has 2048 pixels, which cover a 250 nm wavelength range with a line scan rate of up to 70 kHz at a 12 bit resolution. Spectral resolution of 0.12 nm determines an imaging depth of 1.23 mm, while the system detection sensitivity and roll-off were measured to be −108 dB (at an incident power of ~9 mW) and −16 dB (over the 1.23 mm imaging depth), respectively.

In the sample arm, an endoscopic catheter (~1.5 m long) with diffractive optics at distal end was used to minimize the chromatic aberrations over the broadband spectrum [14]. The endoscopic catheter of 1.27 mm outer diameter (including the protective metal guard) was inserted into a transparent protective plastic sheath of 1.78 mm outer diameter. Detailed design of the diffractive catheter can be found in [14]. A prism pair with SF11 flint glass was inserted in the free space of the reference arm to carefully match the dispersion between sample and reference arms. SF11 flint glass has a high group velocity and third-order dispersion and can effectively minimize the dispersion mismatch between the two arms while keeping sufficient free space (air gap) in the reference arm. Furthermore, the polarization state of the sample and reference arm was carefully managed by using polarization controllers to maximize the interference fringe contrast. Figure 2(c) shows the measured point-spread function (PSF) of the system. Through the combination of the home-built broadband rotary joint described above and the diffractive catheter, the chromatic aberration was effectively minimized, enabling us to achieve an ultrahigh axial resolution of ~2.4 μm in air (~1.7 μm in tissue), where the theoretical axial resolution is about 2.0 μm assuming a perfect Gaussian source spectrum.

Finally, *in vivo*, high-speed, ultrahigh-resolution endoscopic OCT imaging was demonstrated with the broadband rotary joint. The entire rotary joint assembly was mounted on a motorized translational stage to perform pull-back during circumferential scanning to acquire 3D volumetric images. The experiment was conducted under an imaging protocol approved by the Animal Care and Use Committee at the Johns Hopkins University. Total optical power to the interferometer was adjusted before the experiment by a polarizer [indicated by PL in Fig. 2(a)], ensuring the output power at the catheter tip was ~9 mW.

Figure 3(a) shows a cutaway view of the reconstructed 3D image with 1200 consecutive cross-sectional images of a mouse colon and rectum. Cross-sectional images were acquired at 20 fps, with each frame consisting of 3500 A-lines. Three-dimensional volumetric imaging was performed by pulling back the catheter at a speed of 0.4 mm/s (corresponding to an imaging pitch of 20 μm) during continuous circumferential rotation. Figure 3(b) shows a representative cross-sectional image of a mouse rectum. A 3× zoomed-in image and the representative histology are shown, respectively, in Figs. 3(c) and 3(d), with good correlation to each other. Fine microstructures such as muscularis mucosae, submucosa, muscularis interna, and muscularis externa can be clearly identified. The crypts structure in the first layer of the mucosa can also be appreciated; however, with a suboptimal contrast, which could be due to the compression of the tissue surface in direct contact with the plastic sheath

of the catheter and the small size of the imaged lumen. Those contextures can be much more clearly seen in an *en face* projection view of the 3D image. Figures 3(e)–3(g) show the projection view, and the cross-sectional views along the radial and longitudinal (pull-back) directions (with the directions indicated by the dashed lines) in Fig. 3(e), respectively. The projection image was constructed by summation of the OCT intensity along the imaging depth, with a field of view of 4.8 mm × 1.23 mm × 5 mm (radial × depth × longitudinal). The crypts are pronounced, as shown in the enlarged inset of Fig. 3(e).

In summary, we have developed a broadband rotary joint with enhanced robustness for high-speed and ultrahigh-resolution imaging at 800 nm. The rotary joint utilizes custom five-axis kinematic mounts to ensure precise alignment and mechanical robustness. Achromatic doublets were used to effectively minimize the chromatic aberration over the broad spectral bandwidth centered around 800 nm, enabling us to achieve an ultrahigh axial resolution of 2.4 μm (in air). Compared with bare fiber couplers, the robust mechanical design in the reported rotary joint allows long-lasting imaging at a near video-rate (20 fps) for real-time applications. Higher speeds can be achieved in the future by further miniaturizing the current assembly (including the kinematic mounts and doublets).

Acknowledgments

Funding. National Institutes of Health (NIH) (R01CA153023, R01HL121788); Wallace H. Coulter Foundation (WHCF); Maryland Innovation Initiative (TEDCO-MII).

References

1. Tearney GJ, Brezinski ME, Bouma BE, Boppart SA, Pitris C, Southern JF, Fujimoto JG. Science. 1997; 276:2037. [PubMed: 9197265]
2. Jing J, Zhang J, Loy AC, Wong BJF, Chen Z. J Biomed Opt. 2012; 17:110507. [PubMed: 23214170]
3. Armstrong JJ, Leigh MS, Walton ID, Zvyagin AV, Alexandrov SA, Schwer S, Sampson DD, Hillman DR, Eastwood PR. Opt Express. 2003; 11:1817. [PubMed: 19466064]
4. Adler DC, Zhou C, Tsai TH, Schmitt J, Huang Q, Mashimo H, Fujimoto JG. Opt Express. 2009; 17:784. [PubMed: 19158891]
5. Bouma BE, Tearney GJ, Compton CC, Nishioka NS. Gastrointestinal Endosc. 2000; 51:467.
6. Xi J, Huo L, Wu YC, Cobb MJ, Hwang JH, Li XD. Opt Lett. 2009; 34:1943. [PubMed: 19571960]
7. Fu HL, Leng YX, Cobb MJ, Hsu K, Hwang JH, Li XD. J Biomed Opt. 2008; 13:060502. [PubMed: 19123643]
8. Tran PH, Mukai DS, Brenner M, Chen ZP. Opt Lett. 2004; 29:1236. [PubMed: 15209258]
9. Herz PR, Chen Y, Aguirre AD, Schneider K, Hsiung P, Fujimoto JG, Madden K, Schmitt J, Goodnow J, Petersen C. Opt Lett. 2004; 29:2261. [PubMed: 15524374]
10. Tsai TH, Lee HC, Ahsen OO, Liang K, Giacomelli MG, Potsaid BM, Tao YK, Jayaraman V, Figueiredo M, Huang Q, Cable AE, Fujimoto J, Mashimo H. Biomed Opt Express. 2014; 5:4387. [PubMed: 25574446]
11. Bouma B, Tearney GJ, Boppart SA, Hee MR, Brezinski ME, Fujimoto JG. Opt Lett. 1995; 20:1486. [PubMed: 19862057]
12. Drexler W, Morgner U, Ghanta RK, Kartner FX, Schuman JS, Fujimoto JG. Nat Med. 2001; 7:502. [PubMed: 11283681]
13. Yuan W, Mavadia-Shukla J, Xi J, Liang W, Yu X, Yu S, Li XD. Opt Lett. 2016; 41:250. [PubMed: 26766686]
14. Xi J, Zhang A, Liu Z, Liang WX, Lin LY, Yu S, Li XD. Opt Lett. 2014; 39:2016. [PubMed: 24686663]

15. Cho HS, Jang S-J, Kim K, Dan-Chin-Yu AV, Shishkov M, Bouma BE, Oh W-Y. Biomed Opt Express. 2014; 5:223.
16. Li XD, Chudoba C, Ko T, Pitris C, Fujimoto JG. Opt Lett. 2000; 25:1520. [PubMed: 18066265]
17. Hu Z, Rollins AM. Opt Lett. 2007; 32:3525. [PubMed: 18087530]

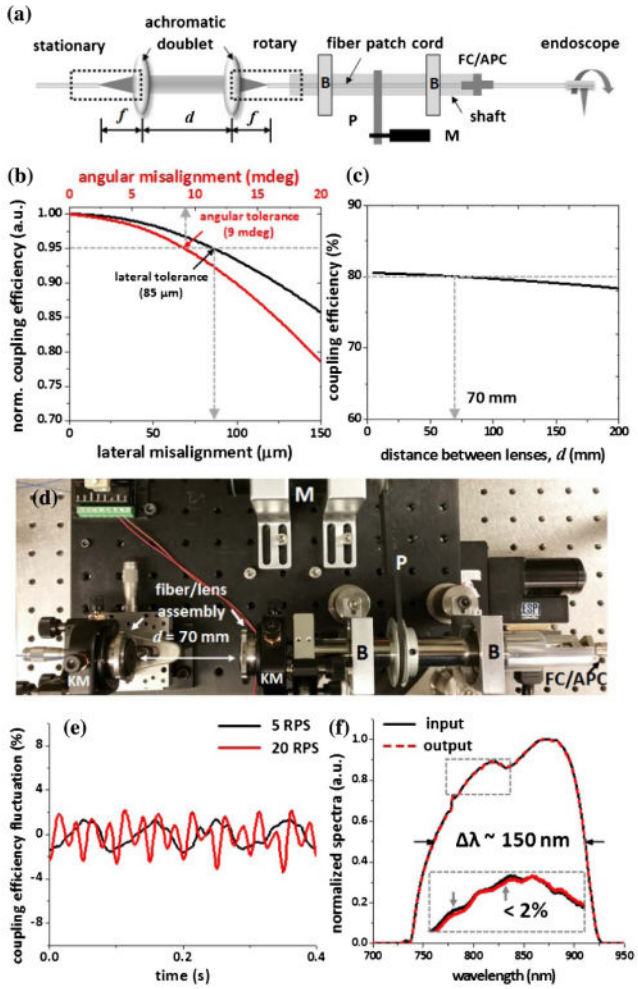

Fig. 1.

(a) Schematic of the broadband rotary joint. (b) and (c) Tolerance analysis on coupling efficiency of the broadband rotary joint; less than ±5% coupling efficiency fluctuation can be achieved within alignment tolerance of ±85 μm (lateral misalignment) or ±9 mdeg (angular misalignment) (b), while providing over 80% of one-way throughput at a maximum separation of 70 mm between the two lenses (c). (d) Photograph of the assembled broadband rotary joint. (e) Intensity throughput fluctuation of the broadband rotary joint at two representative rotation speeds. (f) Comparison of the input and output spectrum of the broadband rotary joint; maximum spectrum variation was less than 2% (see the inset). B, bearing; M, DC motor; P, pulley; KM, five-axis kinematic mount.

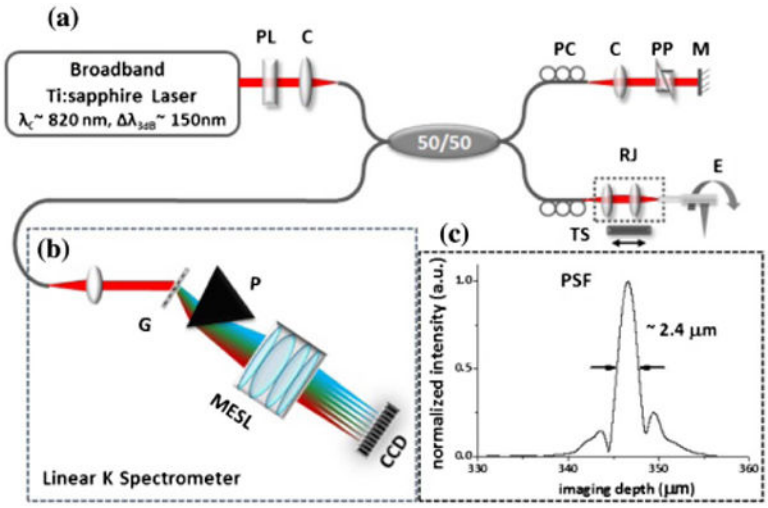

Fig. 2.

(a) Schematic of the ultrahigh-resolution endoscopic SD-OCT imaging system with the broadband rotary joint and diffractive-optics-based catheter. (b) Schematic of the home-built linear-wavenumber spectrometer. (c) Measured axial point-spread function (PSF) of the system; chromatic aberrations were effectively managed, and the axial resolution of ~2.4 μm (in air) was achieved. CCD, line scan CCD; C, collimator; G, grating; M, mirror; MESL, multi-element scan lens; P, linear K mapping prism; PC, polarization controller; PL, polarizer; PP, dispersion compensating prism pair; RJ, fiber-optic rotary joint; TS, motorized translational stage.

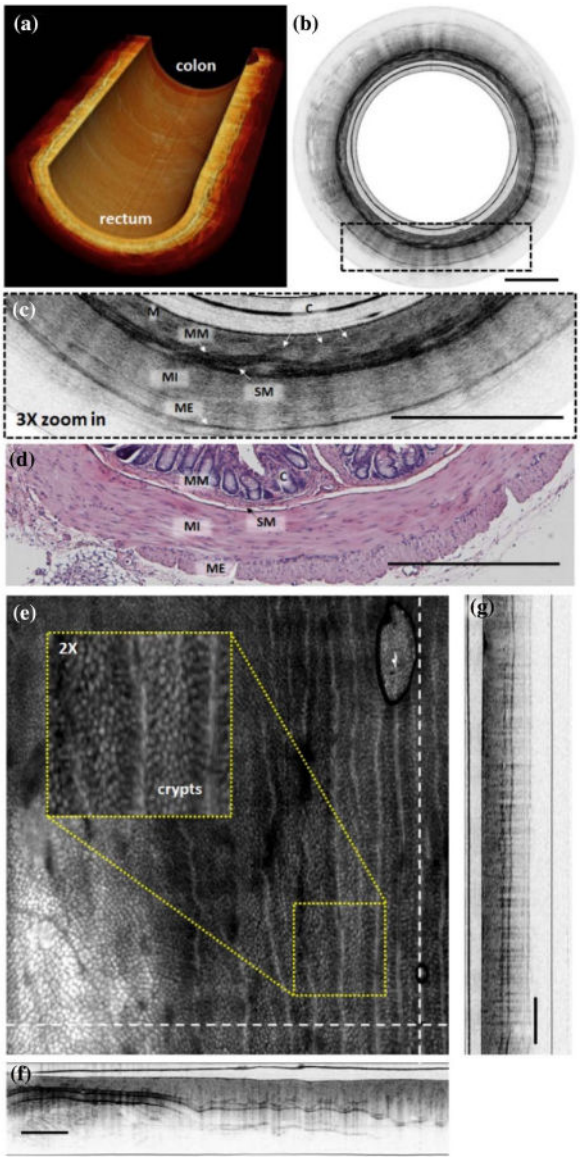

Fig. 3.

(a) Cutaway view of a reconstructed 3D OCT image of a section of mouse colon and rectum along a 2.4 cm catheter pull-back distance with a 20 μm pitch at 20 fps. (b) Representative cross-sectional image of mouse rectum. (c) 3× zoomed-in region of the dotted box in (b), with a representative histology micrograph shown in (d). (e) *En face* projection image constructed by axial intensity summation over a 4.8 mm × 1.23 mm × 5 mm radial × depth × pull – back) field of view. Crypts and vessel structures are more readily visible. Inset: Enlarged view of the yellow box region. (f)–(g) Cross-sectional image along the dashed lines in (e), which correspond to the radial and longitudinal (pull-back) direction, respectively. M, mucosa; MM, muscularis mucosae; SM, submucosa; MI, muscularis interna; ME, muscularis externa; C, crypts. Scale bar is 500 μm.